



Published in final edited form as:

ASAIO J. 2017 ; 63(2): 216–222. doi:10.1097/MAT.0000000000000463.

## Development of a Model of Pediatric Lung Failure Pathophysiology

John M. Trahanas<sup>1,2</sup>, Fares Alghanem<sup>1</sup>, Catalina Ceballos-Muriel<sup>1,3</sup>, Hayley R. Hoffman<sup>1</sup>, Alice Xu<sup>1</sup>, Kristopher B. Deatruck<sup>1,4</sup>, Marie Cornell<sup>1</sup>, Alvaro Rojas-Pena<sup>1,5</sup>, Robert H. Bartlett<sup>1</sup>, and Ronald B. Hirschi<sup>1,6</sup>

<sup>1</sup>Extracorporeal Life Support Laboratory, Department of Surgery, University of Michigan Medical School, Ann Arbor, MI, USA

<sup>2</sup>Department of Surgery, Columbia University Medical Center, New York, NY, USA

<sup>3</sup>Department of Surgery, Universidad el Bosque – Escuela Colombiana de Medicina, Bogota, Colombia

<sup>4</sup>Department of Cardiac Surgery, University of Michigan, Ann Arbor, MI, USA

<sup>5</sup>Department of Surgery, Section of Transplant Surgery, University of Michigan Health Systems, Ann Arbor, MI, USA

<sup>6</sup>Department of Surgery, Section of Pediatric Surgery, University of Michigan Health Systems, Ann Arbor, MI, USA

### Abstract

A pediatric artificial lung (PAL) is under development as a bridge to transplantation or lung remodeling for children with end-stage lung failure (ESLF). In order to evaluate the efficiency of a PAL, a disease model mimicking the physiologic derangements of pediatric ESLF is needed. Our previous right pulmonary artery ligation (rPA-LM) ovine model achieved that goal, but caused immediate mortality in nearly half of the animals. In this study, we evaluated a new technique of gradual postoperative right pulmonary artery (rPA) occlusion using a Rummel tourniquet (rPA-RT) in seven (25–40 Kg) sheep. This technique created a stable model of ESLF pathophysiology, characterized by high alveolar dead space (58.0±3.8 %), pulmonary hypertension (38.4±2.2 mmHg), tachypnea (79±20 breaths per minute), and intermittent supplemental oxygen requirement. This improvement to our technique provides the necessary physiologic derangements for testing a PAL, while avoiding the problem of high immediate perioperative mortality.

### Keywords

Lung failure; animal model; pulmonary hypertension

---

Address for Correspondence: Alvaro Rojas-Pena, MD, Extracorporeal Life Support Laboratory - Department of Surgery, University of Michigan, 1150 W. Medical Center Drive, B560 MSRBII/SPC 5686, Ann Arbor, MI 48109, alvaror@med.umich.edu, Tel: 734-615-5357, Fax: 734-615-4220.

**Disclaimers:** None

**Conflict of Interests:** The authors declare no conflicts of interest.

## INTRODUCTION

Waiting list mortality for pediatric lung transplantation approaches 25% due to lack of suitable long term bridging options.<sup>1</sup> An implantable pediatric artificial lung (PAL) would be an ideal modality for bridging pediatric patients to lung transplantation as it would allow for participation in physical therapy and therefore potentially lead to improved post transplantation outcomes.<sup>2</sup> Artificial lungs designed specifically to meet the needs of the pediatric population are being developed. In order to test these new designs, animal models that mimic the physiologic derangements observed in pediatric patients with end-stage lung failure (ESLF) are required.

The diseases most frequently requiring transplantation in the pediatric population include cystic fibrosis, idiopathic pulmonary artery hypertension, congenital diaphragmatic hernia with associated pulmonary hypoplasia and pulmonary hypertension, idiopathic pulmonary fibrosis, obliterative bronchitis, and bronchopulmonary dysplasia.<sup>3,4</sup> These conditions, while differing in etiology and medical therapy, each display at least some of the following physiologic characteristics: pulmonary artery hypertension with associated right ventricular (RV) failure, impaired oxygenation, increased dead space fraction, and respiratory distress causing growth and exercise limitation.<sup>5,6</sup> As such, an artificial lung designed for pediatric use must be effective in addressing these pathophysiologic derangements if it is to be sufficiently versatile for use in all the aforementioned conditions.

Our previous right pulmonary artery (rPA) ligation model (rPA-LM) was successful in achieving the pathophysiologic requirements, but was plagued by high rates of fatal perioperative RV failure.<sup>7</sup> In this study, we introduced a major modification of our methods to induce rPA occlusion after full recovery from the thoracotomy and anesthesia using a Rummel tourniquet (rPA-RT). This new method allows for successful recovery of the animals, followed by slow and reversible titration of the rPA occlusion until full occlusion is achieved. We compared the pathophysiology generated by this new model against our published rPA-LM model.<sup>7</sup>

## Methods

All animals received humane care in accordance with the NIH Guide for the Care and Use of Laboratory Animals. Animal protocols were approved by the University of Michigan Institutional Animal Care and Use Committee (IACUC).

### Baseline Data Collection

Fourteen animals were used, divided into two groups of seven animals each: rPA-LM and rPA-RT. Baseline instrumentation was identical to our previous published methods.<sup>7</sup> Briefly, healthy lambs (25–40 Kg) were anesthetized, intubated, and mechanically ventilated at a frequency of 12 breaths per minute and tidal volume of 15 mL/Kg. Each animal had arterial, venous, and oximetric pulmonary arterial catheters placed (which were left in place postoperatively for data collection), and baseline arterial and venous blood gases and hemodynamics were recorded. Baseline dead space ventilation fraction measurements were

also conducted with a modified ventilation circuit (calculated using the Bohr-Enghoff equation).<sup>8</sup>

### Occlusion Devices

1. Hem-O-Lok Clip: A commercially available vascular occlusion clip (TeleFlex, Morrisville, NC) designed to seal large vessels, applied acutely to the rPA (**rPA-LM group**).
2. Rummel tourniquet: A soft silicon rubber 8Fr pediatric feeding tube (Bard, Covington, GA) was passed around the right pulmonary artery. To create our Rummel occlusion device we amputated the distal aspect of 20Fr thoracostomy tube (Covidien, Dublin, IE) to remove all side holes. The soft silicon rubber tube was snared through the thoracostomy tube. The device was then tunneled through the skin (**rPA-RT group**).

### Operative Procedure

The rPA-LM animals had a Hemo-O-Lok clip placed as previously described.<sup>7</sup> For the new set of animals, the same left thoracotomy was performed, and the left and right branches of the main pulmonary artery dissected. The occlusion device, which consisted of a flexible Rummel tourniquet device (rPA-RT) was placed around the rPA. The device was tunneled out of the chest and through the skin, and was then tightened until full occlusion. Once full occlusion was visually confirmed, hemodynamics and arterial and venous blood gases were documented. Post-occlusion dead space fraction was then determined. The occlusion device was then released until pulmonary artery pressures returned to baseline. A 20Fr thoracostomy tube was placed in the pleural space to  $-20$  mmHg suction. Lidocaine (0.5%, 60 mL) was administered as an intercostal nerve block over ribs 3–7. The chest was then closed; and the animal recovered, extubated, and transferred to a restraining cage in our sheep intensive care unit (shICU).

### Postoperative Care

In our shICU, animals were under 24/7 care by laboratory personnel. Hemodynamics were monitored continuously and recorded hourly. Arterial and mixed venous blood gases recorded every 6 hours, or more frequently if deemed necessary. Animals received antibiotics and PRN pain control according to our established animal protocols.<sup>7</sup> Supplemental oxygen, when needed, was administered via nasal cannula and titrated to an arterial saturation of  $>92\%$ . Thoracostomy tubes were removed according to standard clinical criteria.

### Occlusion Protocol

On POD 1 the delayed occlusion model (rPA-RT) animals were evaluated for occlusion eligibility. Eligibility requirements for inducing occlusion included: (1) stable vital signs and normal hemodynamic parameters, (2) freedom from supplemental oxygen via nasal cannula for  $>12$  hours, (3) arterial and venous blood gas values within the normal range, (4) stable hemoglobin levels and normal electrolytes, (5) normal level of alertness, food and water intake, and urine output. During initial occlusion blood pressure, pulmonary artery pressure

( $P_{PA}$ ), and cardiac output were monitored meticulously. The occlusion device was tightened slowly over several minutes until the premarked level (rPA-RT) was achieved, and predetermined intraoperative occlusion pressures confirmed. While tightening, if mean arterial pressure decreased to  $<50$  mmHg or if cardiac output decreased to  $<2.5$  L/min, the occlusion device was loosened until those values were achieved. The occlusion device was then tightened slowly over the following 12 hours until full occlusion based on predetermined intraoperative pulmonary pressures could be achieved. After full occlusion, animals were maintained in our shICU for up to 7 post-occlusion days. The experiment was terminated early if the animal met any of the following predetermined criteria:

- Lactate:  $> 10$  mmol/L once or  $> 5$  mmol/L persistently
- Partial pressure of arterial carbon dioxide ( $PaCO_2$ ):  $> 60$  mmHg on greater than two measurements in 6 hours
- Arterial oxygen saturation ( $SaO_2$ ):  $< 90\%$  despite 4 L/min  $O_2$  for greater than 4 hours
- Mixed venous oxygen saturation ( $SvO_2$ ):  $< 30\%$  despite 4 L/min  $O_2$  for greater than 4 hours
- Significant respiratory distress as judged by the clinical care team

### Statistical Analysis

Survival analysis between groups was performed using a Log Rank test of the Kaplan-Meier survival curves. Changes in dead space fraction and intraoperative  $PaCO_2$  were analyzed using a paired Student t-test to compare each model's pre- and postocclusion values and were analyzed using a Mann-Whitney U-test to compare the difference in percent increase between groups. For all other variables, Mann-Whitney U-test analysis was used to compare the overall mean post-rPA occlusion values of the different disease models. Additionally, each model's preocclusion baseline was compared to its postocclusion values via a repeated measures linear mixed model. Each individual animal's daily variable average was used as a separate repeated measurement. Hemodynamic variables used intraoperative measurements as baseline, respiratory variables used postoperative, preocclusion measurements as baseline. For the purposes of statistical analysis, because the rPA-LM lacks nonoccluded postoperative baseline values, its intraoperative baseline was used as a surrogate. All analysis was performed in SPSS 23 (IBM, Armonk, NY) with p-values  $<0.05$  considered significant. Values are reported and graphed as means  $\pm$  standard deviations.

### Results

After intraoperative full occlusion, with animals sedated and mechanically ventilated, we observed significant increases from baseline in dead space fraction ( $V_d/V_t$ ) and arterial  $PCO_2$  ( $PaCO_2$ ) in both models (Figure 1). Overall (n=14) average  $V_d/V_t$  increased from  $0.47 \pm 0.07$  to  $0.59 \pm 0.04$  ( $p < 0.001$ ) and average  $PaCO_2$  increased from  $41.4 \pm 7.6$  to  $52.6 \pm 7.1$  mmHg ( $p < 0.001$ ). There were no significant differences in the percent increase from baseline between groups with regard to  $V_d/V_t$  ( $p = 0.935$ ) nor  $PaCO_2$  ( $p = 0.573$ ).

Inducing occlusion remote from anesthesia (rPA-RT) was effective in reducing both early mortality (defined as mortality within 24 hours of occlusion) and overall mortality (defined as mortality within 7 days of occlusion) (Figure 2). The rPA-RT model had lower early mortality (0% vs. 71%,  $p < 0.001$ ) and overall mortality compared to rPA-LM (715 VS. 100%,  $p = 0.005$ ).

In the rPA-RT model, after releasing the occlusion devices intraoperative mean pulmonary artery pressures ( $P_{PA}$ ) returned to normal and all seven animals were recovered from anesthesia and extubated to room air. The following day, when the animals were fully recovered, occlusion was again induced. All animals tolerated full occlusion within twelve hours of the first occlusion attempt. While transient changes in arterial blood pressure were observed, trends show no significant changes from baseline values over the course of the experiment in the rPA-LM ( $p = 0.536$ ) and only a small change in the rPA-RT model ( $p = 0.020$ ) (Figure 3A).

After occlusion, the  $P_{PA}$  significantly increased from intraoperative baseline to  $>25$  mmHg in both disease model groups. (rPA-LM  $17.4 \pm 2.2$  vs.  $27.2 \pm 2.3$  mmHg,  $p = 0.001$ ; rPA-RT  $20.4 \pm 3.9$  vs.  $39.4 \pm 6.4$  mmHg,  $p = 0.001$ ). rPA-RT animals achieved significantly higher postoperative  $P_{PA}$  ( $39.4 \pm 6.4$  mmHg) than the rPA-LM group ( $p = 0.008$ ) (Figure 3B).

When cardiac output was directly measured by oximetric catheter, there were no statistically significant differences from intraoperative baseline (rPA-LM  $p = 0.678$ ; rPA-RT  $p = 0.083$ ) nor between groups ( $p = 0.439$ ) (Figure 3C). Similarly, there were no significant differences in  $SvO_2$  between postoperative baseline and postocclusion (rPA-RT  $50.2 \pm 5.5$  vs.  $41.7 \pm 8.9$  %,  $p = 0.222$ ) (Figure 3D).

Tachypnea (average respiratory rate  $>40$  bpm) was observed in all disease model animals, these values are plotted on Figure 4A. There was a significant difference between postoperative baseline and postocclusion in the rPA-RT model (rPA-RT  $p = 0.043$ ). (This variable cannot be assessed under mechanical ventilation, thus no analysis was performed for the rPA-LM model). Hypercapnea induced by increased dead space was compensated by tachypnea in both groups (Figures 4B). There were no significant differences between models ( $p = 0.186$ ) nor between postoperative baseline and postocclusion  $P_{aCO_2}$ . (rPA-RT  $35.0 \pm 2.4$  vs.  $38.1 \pm 4.2$  mmHg,  $p = 0.094$ ).

Supplemental oxygen was routinely required to maintain arterial oxygen saturations above 92% in both groups (Figure 4C and 4D). In animals requiring it,  $P_{aO_2}$  immediately prior to supplemental oxygen was  $59 \pm 7$  mmHg. Average requirement was rPA-LM  $2.0 \pm 2.8$  L/min and rPA-RT  $1.0 \pm 1.3$  L/min. There were no significant differences between the models ( $p = 0.278$ ). Average  $P_{aO_2}$  with supplemental oxygen was rPA-LM  $110 \pm 16$  mmHg and rPA-RT  $78 \pm 3$  mmHg ( $p = 0.003$ ).

The causes of death in the rPA-LM group was perioperative RV failure ( $n = 3$ ), and postoperative cardiorespiratory failure ( $n = 4$ ). The causes of death in the rPA-RT group were all due to cardiorespiratory failure ( $n = 5$ ). The specific indications for early study termination in the rPA-RT group were hypercapnea ( $n = 1$ , endpoint  $P_{aCO_2}$  57.5 mmHg with significant animal discomfort), cardiopulmonary collapse due to RV failure ( $n = 2$ , endpoint lactate

between 9.9–11.5 mmol/L), or significant increases in supplemental oxygen requirement (n=2, endpoint O<sub>2</sub> requirement 8 L/min).

## Discussion

Testing of a pediatric artificial lung requires a reproducible disease model in order to demonstrate effectiveness. Adult lung disease is often characterized by a long-standing inflammatory process, whereas pediatric ESLF is often a result of a developmental disease. Given that pediatric ESLF is not characterized by a systemic inflammatory response, it is our opinion that commonly used adult models which induce lung injury via inflammatory mechanisms such as smoke inhalation or saline lavage are not suitable as pediatric ESLF models.<sup>9, 10</sup> Beading or injection of glues into the pulmonary vasculature is an alternative. Our group has used this method in the past and can attest that it is a longer and more tedious process with an imprecise and unreliable degree of physiologic derangement that is highly variable and often not reproducible.<sup>11–13</sup> It can be difficult to find the ideal dosing of embolic material as too little will often not cause disease, and too much will result in high mortality. For this reason, we strove to develop an acute and reliable method to induce sustained pulmonary hypertension with respiratory dysfunction (and without inflammation), and eventually settled on the technique of acute rPA ligation. Our previous model was effective in meeting our physiologic goals, but had an unacceptably high rate of immediate postoperative mortality thought to be due to the challenge of recovering from anesthesia in the face of acute RV dysfunction.<sup>7</sup>

Other groups have documented a similar approach, utilizing left PA ligation or embolization to mimic chronic thromboembolic pulmonary hypertension.<sup>14, 15</sup> Those methods were successful in creating chronic lung ischemia, but not persistent pulmonary hypertension. It has been shown that more than half of the pulmonary vasculature must be obstructed to create a significant increase in pulmonary vascular resistance.<sup>16</sup> Because of the higher percentage flow to the larger right lung, ligating the left PA alone was inadequate. These models required coupling with weekly and expensive endovascular embolization of right lower lobe pulmonary artery branches to achieve a significant degree of pulmonary hypertension.<sup>16, 17</sup> Weekly embolization has an advantage by training the RV to handle increased pressures over time, allowing for RV remodeling and thus reduces mortality from acute RV failure.<sup>18</sup> These investigators were able to demonstrate that, after two weeks, their model animals exhibited characteristics typical of patients with chronically increased PA pressures including: RV hypertrophy and enlargement, paradoxical septal motion on echocardiogram, distal postobstructive pulmonary vasculopathy, increased systemic blood supply to the obstructed territories, and lesions in the vasculature of vessels in unobstructed territories.<sup>16</sup>

Our model produces a similar degree of P<sub>PA</sub> as do the models of Fadel et al. We would expect to see similar changes in the architecture of hearts and lungs of our disease model animals if sustained for several weeks. However, our goal was to develop an acute model for the testing of a PAL. Thus, our model caused immediate and sustained increase in P<sub>PA</sub> in a short period of time. Due to the acuity of our model, we did not expect to see significant change in tissue architecture on pathology. The high degree of acuity also increased the

mortality of our original rPA-LM model, as an untrained RV was suddenly subjected to high pulmonary vascular resistance.<sup>18</sup> This phenomenon was likely exacerbated by potential adverse cardiac effects from anesthetics and the need to recover from anesthesia, leading to 43% immediate mortality in the rPA-LM group.<sup>7</sup>

In order to reduce immediate postoperative mortality, we sought to separate the anesthetic insult from disease induction. Initially, we used a commercially available perivascular occlusion device (Harvard Apparatus; Holliston, MA) similar to the adjustable pulmonary artery bands developed in the 1970s to limit pulmonary blood flow in children with left to right cardiac shunts. These devices would allow delayed occlusion, and could be inflated via a subcutaneous port such that no portion of the device needed to exit the skin.<sup>19</sup> During postoperative occlusion, these devices produced transient physiologic derangements, but symptoms would resolve within 24 hours and all animals recovered and survived the study. On necropsy, it was often found that the perivascular balloons had malfunctioned (either leaking or the inflated volume herniated upwards from the band and away from the vessel) and were no longer occluding the rPA.

The rPA-RT model proved to be a reliable method of inducing complete occlusion in the postoperative period, and resulted in the desired disease model. The rPA-RT model also demonstrated more severe physiologic derangement with significantly higher mean  $P_{PA}$ , lower  $PaO_2$ , and trends toward lower  $SvO_2$  compared to the rPA-LM immediate occlusion model. One would expect the rPA-RT animals to have physiologic effects identical to the rPA-LM animals. We suspect that higher mean  $P_{PA}$  and lower  $SvO_2$  were achieved in rPA-RT animals because rPA-LM animals that developed sudden high mean  $P_{PA}$  died immediately from RV failure during recovery from anesthesia. Thus, surviving rPA-LM animals only included those with low  $P_{PA}$  values. In contrast, the rPA-RT animals demonstrated severe physiologic insult, however the insult was survivable after full recovery from anesthesia, and when induced over the course of hours rather than instantly. An advantage of the rPA-RT approach in terms of artificial lung research is that the injury is delayed and controlled which allows a window to attach and evaluate an artificial lung.

While pulmonary hypertension is a large component of the rPA-RT model, the detrimental effect we would expect to see from pure pulmonary hypertension (ie. right ventricular failure and decreased cardiac output) did not occur to a significant degree. The V/Q mismatch and increased dead space created by occluding only the right pulmonary artery is what is key in making this a model of ESLF, rather than purely of pulmonary hypertension. If we were to have decreased the diameter of both right and left pulmonary arteries equally to generate the same amount of pulmonary hypertension without occluding either vessel, we would not expect that V/Q matching would be maintained, as both lungs would still be equally perfused. The increased dead space is responsible for the tachypnea, which was observed in both models, as it was necessary for animals to increase their minute ventilation in order to maintain normocapnea. Even while severely tachypneic, rPA-LM and rPA-RT animals had  $PaCO_2$  values close to 40 mmHg. In the OR, while anesthetized and mechanically ventilated, the underlying hypercapnea was evident upon rPA occlusion. The rPA-RT sheep also developed mild hypoxia with oxygen requirement, which is desirable in a model of ESLF physiology. Death resulted from a combination of respiratory failure when tachypnea

could not compensate for hypercapnea and sudden cardiovascular collapse most likely due to right ventricular failure and arrhythmia. We would postulate that the artificial lung will ameliorate both of these problems, and result in 100% survival in this model.

While the newly described rPA-RT disease model does not represent any particular disease process with high fidelity, the disease model incorporates the most clinically important pathophysiologic characteristics of disorders such as bronchopulmonary dysplasia and congenital diaphragmatic hernia that commonly lead to lung transplantation in the pediatric population. We also acknowledge that our model by design is induced acutely. Thus the chronic adaptations that develop in children who suffer many years of lung disease, such as RV remodeling and pulmonary vasculopathy, will be absent. Our goal was to create a model that *mimics* the pathophysiology of end stage lung failure in which to test artificial lung devices. As such, we accept the shortcoming of not having induced chronic change. For this reason we did not send pathologic specimens nor examine markers of vascular remodeling such as ET-1 as other authors have done.<sup>18, 20</sup>

## Conclusions

In this study, we were able to generate an acute model of ESLF physiology. The rPA-RT model demonstrates persistent pulmonary hypertension with decreased mixed venous saturation and respiratory distress defined by tachypnea and mild hypoxia. We believe that the rPA-RT approach will serve as an inexpensive and reproducible method to test the effectiveness of the pediatric artificial lung.

## Acknowledgments

**Funding:** National Institute of Child Health and Human Development (US) Grant 2RO1 HD015434-29

We thank the tireless students and technicians of the ECLS Lab for their help with care of the animals. We also thank Cindy Cooke for reviewing this manuscript.

## References

1. Valapour M, Paulson K, Smith J, et al. Optn/srtr 2011 annual data report: Lung. American Journal of Transplantation. 2013; 13:149–177. [PubMed: 23237700]
2. Turner DA, Cheifetz IM, Rehder KJ, et al. Active rehabilitation and physical therapy during extracorporeal membrane oxygenation while awaiting lung transplantation: A practical approach. Critical care medicine. 2011; 39:2593–2598. [PubMed: 21765353]
3. Dipchand AI, Kirk R, Edwards LB, et al. The registry of the international society for heart and lung transplantation: Sixteenth official pediatric heart transplantation report—2013; focus theme: Age. The Journal of Heart and Lung Transplantation. 2013; 32:979–988. [PubMed: 24054806]
4. Kinsella JP, Greenough A, Abman SH. Bronchopulmonary dysplasia. The Lancet. 2006; 367:1421–1431.
5. Dishop MK. Paediatric interstitial lung disease: Classification and definitions. Paediatric respiratory reviews. 2011; 12:230–237. [PubMed: 22018036]
6. Sweet SC. Pediatric lung transplantation. Proceedings of the American Thoracic Society. 2009; 6:122–127. [PubMed: 19131537]
7. Alghanem F, Davis RP, Bryner BS, et al. The implantable pediatric artificial lung: Interim report on the development of an end-stage lung failure model. ASAIO journal (American Society for Artificial Internal Organs: 1992). 2015; 61:453–458. [PubMed: 25905495]



8. Nunn J, Holmdahl MHs. Henrik enghoff and the volumen inefficax. *Upsala journal of medical sciences*. 1978; 84:105–108.
9. Kimura R, Traber L, Herndon D, Linares H, Lubbesmeyer H, Traber D. Increasing duration of smoke exposure induces more severe lung injury in sheep. *Journal of Applied Physiology*. 1988; 64:1107–1113. [PubMed: 3366733]
10. Zick G, Frerichs I, Schädler D, et al. Oxygenation effect of interventional lung assist in a lavage model of acute lung injury: A prospective experimental study. *Critical Care*. 2006; 10:R56. [PubMed: 16606436]
11. Shelub I, van Grondelle A, McCullough R, Hofmeister S, Reeves JT. A model of embolic chronic pulmonary hypertension in the dog. *Journal of Applied Physiology*. 1984; 56:810–815. [PubMed: 6706785]
12. Perkett E, Brigham K, Meyrick B. Continuous air embolization into sheep causes sustained pulmonary hypertension and increased pulmonary vasoreactivity. *The American journal of pathology*. 1988; 132:444. [PubMed: 3414777]
13. Sato H, Hall CM, Griffith GW, et al. Large animal model of chronic pulmonary hypertension. *ASAIO journal*. 2008; 54:396–400. [PubMed: 18645357]
14. Fadel E, Riou JY, Mazmanian M, et al. Pulmonary thromboendarterectomy for chronic thromboembolic obstruction of the pulmonary artery in piglets. *The Journal of thoracic and cardiovascular surgery*. 1999; 117:787–793. [PubMed: 10096975]
15. Fadel E, Michel RP, Eddahibi S, et al. Regression of postobstructive vasculopathy after revascularization of chronically obstructed pulmonary artery. *The Journal of thoracic and cardiovascular surgery*. 2004; 127:1009–1017. [PubMed: 15052197]
16. Mercier O, Tivane A, Dorfmueller P, et al. Piglet model of chronic pulmonary hypertension. *Pulmonary circulation*. 2013; 3:908. [PubMed: 25006407]
17. Tivane A, Raoux F, Decante B, et al. A reliable piglet model of chronic thrombo-embolic pulmonary hypertension. *Am J Respir Crit Care Med*. 2011; 183:A2415.
18. Mercier O, Fadel E. Chronic thromboembolic pulmonary hypertension: Animal models. *European Respiratory Journal*. 2013; 41:1200–1206. [PubMed: 23314897]
19. Edmunds LHJ, Rudy LW, Heymann MA, Boucher JK. An adjustable pulmonary arterial band. *ASAIO Journal*. 1972; 18:217–223.
20. Kim H, Yung G, Marsh J, et al. Endothelin mediates pulmonary vascular remodelling in a canine model of chronic embolic pulmonary hypertension. *European Respiratory Journal*. 2000; 15:640–648. [PubMed: 10780753]

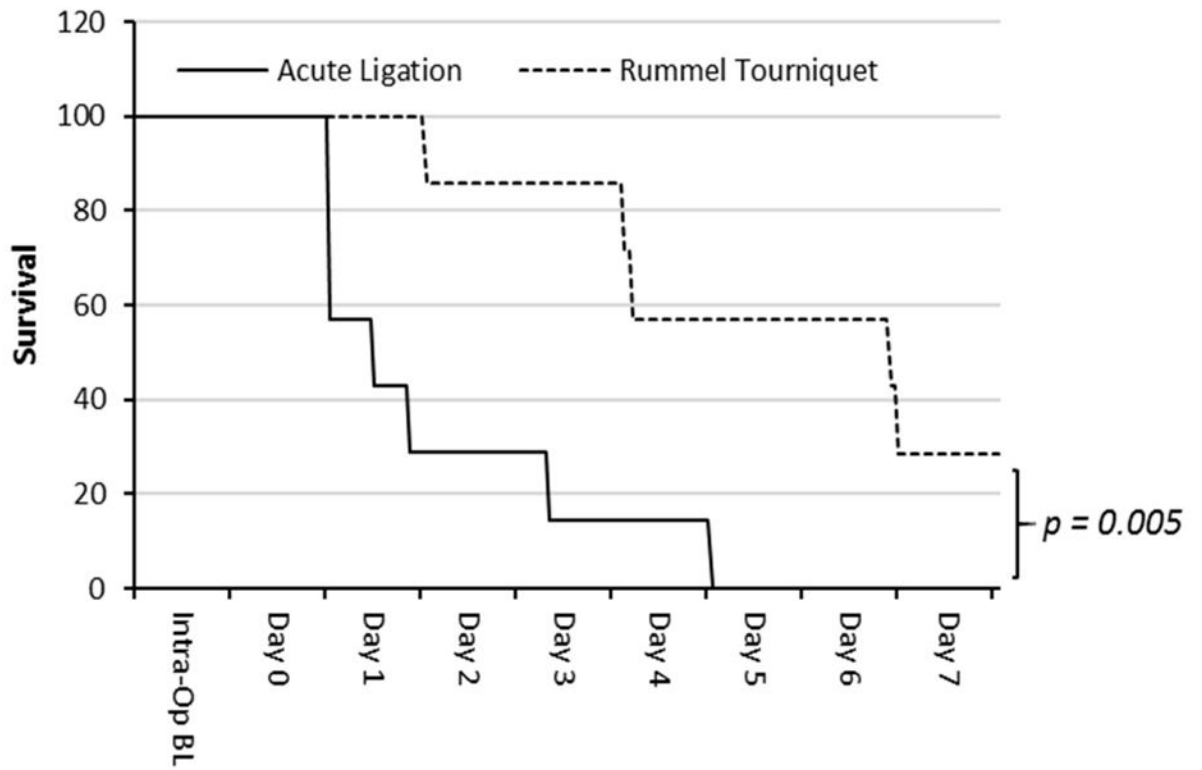


**Figure 1.** Intraoperative values obtained pre and post-occlusion while anesthetized and mechanically ventilated for A) Dead space ventilation fraction and B)  $P_{aCO_2}$

Author Manuscript

Author Manuscript

Author Manuscript

Author Manuscript

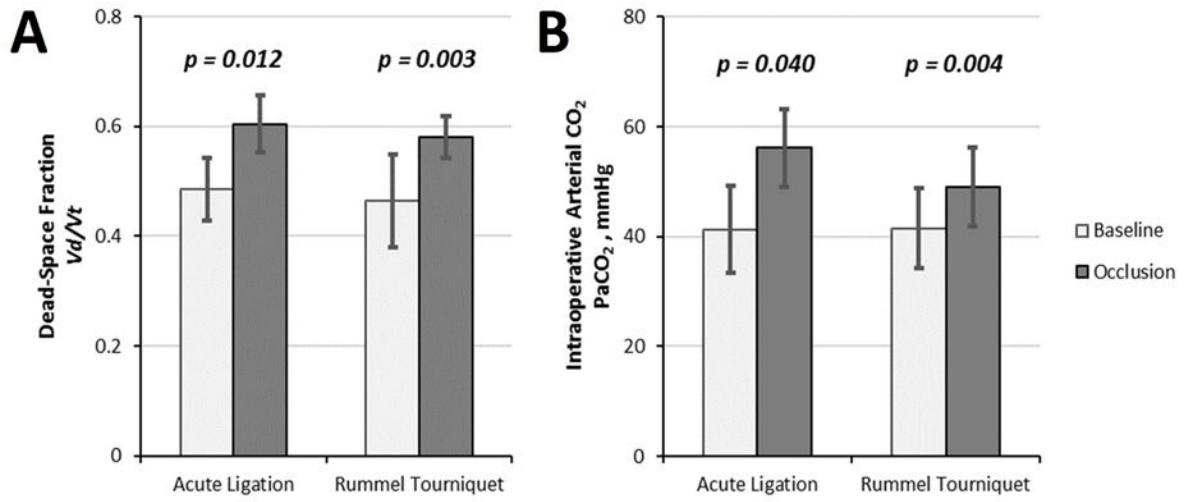


**Figure 2. Kaplan-Meier survival curves**  
 Compared to the rPA-LM group, survival was significantly higher at both day 1 ( $p < 0.001$ ) and day 7 ( $p = 0.005$ ) in the rPA-RT group.

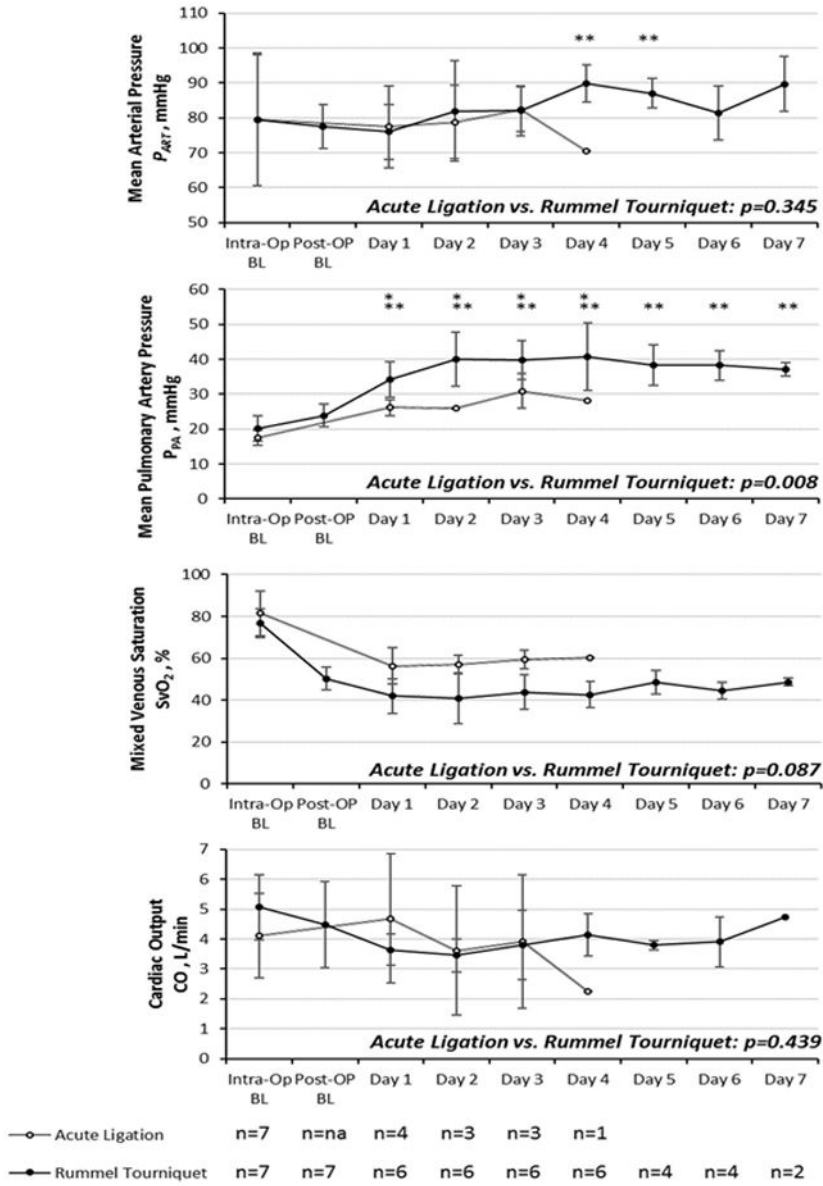


**Figure 3. Hemodynamics plotted over time**

A) Mean arterial blood pressure ( $P_{ART}$ ); B) Mean pulmonary artery pressure ( $P_{PA}$ ); C) Mixed venous oxygen saturation; D) Cardiac output plotted over time. Values are expressed as means  $\pm$  SD. “\*” denotes a significant change from intraoperative baseline in the acute ligation model. “\*\*” denotes a significant change from postoperative baseline in the Rummel tourniquet model.

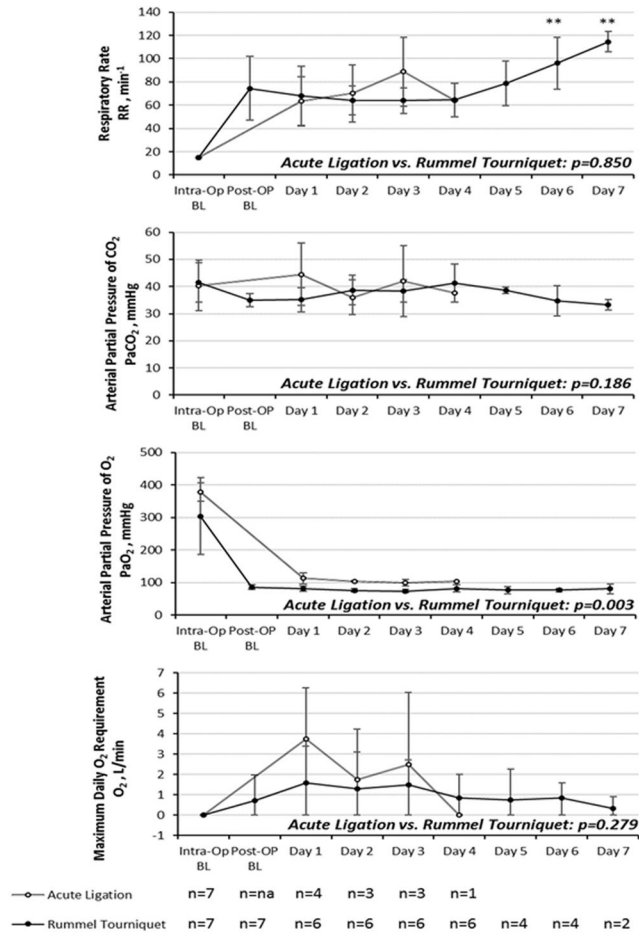


**Figure 4. Respiratory Effects plotted over time**

A) Respiratory rate; B)  $PaCO_2$ ; C)  $PaO_2$ ; D) Average maximum daily oxygen requirement. Values are expressed as means  $\pm$  SD. “\*\*\*” denotes a significant change from postoperative baseline in the Rummel tourniquet model. These variable cannot be assessed under mechanical ventilation, thus no analysis was performed for the rPA-LM model.

**Table 1**

Post-occlusion values and statistical analysis

	rPA-LM <i>n</i> = 7	rPA-RT <i>n</i> = 7	p-value
<b>P<sub>ART</sub>(mmHg)</b>	77±11	84±6	0.345
<b>P<sub>PA</sub>(mmHg)</b>	27±2	39±6	0.008
<b>SvO<sub>2</sub> (%)</b>	52±8	42±9	0.087
<b>Daily Max O<sub>2</sub> Req. (L/min)</b>	2±3	1±1	0.279
<b>PaCO<sub>2</sub>(mmHg)</b>	46±10	38±4	0.186
<b>Respiratory Rate (min<sup>-1</sup>)</b>	70±23	70±17	0.850
<b>Cardiac Output (L/min)</b>	4.5±2.0	3.9±0.5	0.439

Values are expressed as means ± SD. P<sub>ART</sub>, mean arterial pressure; P<sub>PA</sub>, mean pulmonary artery pressure; P<sub>aO<sub>2</sub></sub>, arterial partial pressure of oxygen; SaO<sub>2</sub>, arterial oxygen saturation; SvO<sub>2</sub>, venous oxygen saturation; P<sub>aCO<sub>2</sub></sub>, arterial partial pressure of carbon dioxide